PERFORMANCE ANALYSIS AND DESIGN OF FILTERING HYDROCYCLONES

L. G. M. Vieira, E. A. Barbosa, J. J. R. Damasceno and M. A. S. Barrozo[*]

Universidade Federal de Uberlândia, Faculdade de Engenharia Química,
Phone: +(55) (34) 239-4189, Fax: +(55) (34) 239-4188, Bloco K,
Campus Santa Mônica, CEP 38400-902, Uberlândia - MG, Brazil.
E-mail: masbarrozo@ufu.br

Abstract - The filtering hydrocyclone is a solid-liquid separation device patented by the Chemical Engineering Department at the Federal University of Uberlândia, which consists of a hydrocyclone whose conical section was replaced by a conical filtering wall. The objective of this work is to compare the performances of the filtering hydrocyclones designed by Bradley and by Rietema. The experimental results obtained with the filtering hydrocyclones under the same operational conditions as those used with the conventional device allow the conclusion that performance of the Bradley and Rietema types is significantly influenced by the filtering medium. Rietema's filtering hydrocyclones had a lower volumetric feed flowrate than the conventional device and Bradley's filtering hydrocyclones showed increases in this same variable. In both designs, overall efficiency was influenced by the underflow-to-throughput ratio.
Keywords: Filtering hydrocyclone; Solid-liquid separation; Hydrocyclone.

INTRODUCTION

Hydrocyclones, also known as liquid cyclones, are an important device for the separation of solid-liquid suspensions (Svarovsky, 1984). The principle employed is centrifugal sedimentation, i.e., the particles in the suspension are subjected to centrifugal forces, which causes their separation from the fluid. Like centrifuges, which make use of the same principle, hydrocyclones do not have moving parts, require a low installation and maintenance investment and are simple to operate. Hence, these devices are widely utilized in mineral, chemical, petrochemical, textile and metallurgical industries.

Aiming at combining two separation processes, researchers in the Chemical Engineering Department at the Federal University of Uberlândia proposed a modification of the conventional hydrocyclone (Barrozo et al., 1992). The conical section of a hydrocyclone of Bradley's design was replaced by a conical filtering wall. The resulting equipment was denominated the filtering hydrocyclone.

The hydrocyclone separates solid and liquid or liquid and liquid by the difference in density between the fluid and the material to be separated in this equipment. Due to the fluid acquires a spiraling motion caused by the tangent feeding, the material of larger density is thrown against the wall of the hydrocyclone and dragged to the underflow while the one of smaller density proceeds for the overflow, forming a free vortex (outer vortex) and a forced vortex (inner vortex) in agreement with Figure 1. The filtering hydrocyclone, wich is the subject of this study, has another stream imposed of filtrate originating in the filtration in the conical area. Figure 1 depicts a side view of the filtering hydrocyclone and the trajectory of suspension for the conventional hydrocyclone.

The objective of this work is to compare the performances of filtering hydrocyclones of two different designs, Bradley's and Rietema's (Svarovsky, 1984, Rietema, 1961).

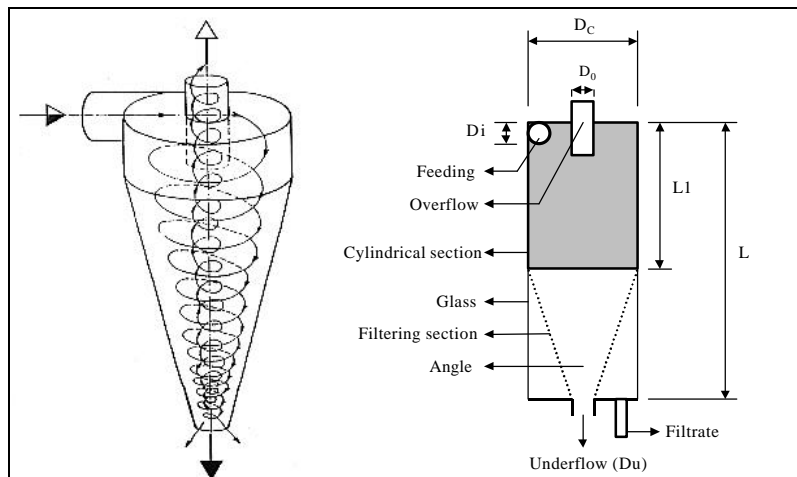---

*To whom correspondence should be addressed

Figure 1: Trajectory of suspension for the conventional hydrocyclone and filtering device scheme

MODELLING

Residence Time Theory

There are several theories for the describing the separation that takes place in hydrocyclones. Perhaps one of the best known is the residence time theory (Svarovsky, 1981). In this approach, first proposed by Rietema (1961), a particle of a given size will be collected if the time it remains inside the cyclone is equal to or greater than the time necessary for it to reach the wall. Under some assumptions, the residence time theory yields Eq.(1) for the prediction of cut size in cyclones:

$$\frac{d_{50}}{D_C} = K\left[\frac{\mu D_C}{Q(\rho_s - \rho)}\right]^{0.5} \tag{1}$$

where d_{50} is the cut size, D_C is the diameter of the cylindrical section of the cyclone, μ is the liquid viscosity, Q is the volumetric feed flowrate, ρ is the liquid density, ρ_s is the solid density and K is a parameter characteristic of each cyclone design, which is usually determined empirically.

It is important to highlight that the cut size obtained during operation of the hydrocyclone results not only from the action of the centrifugal field but also from the solid material carried by the downward stream fluid. Therefore, for the purpose of comparison with other hydrocyclones, the cut size due exclusively to centrifugal separation should be defined. This definition corresponds to the so-called reduced cut size ($d_{50}^{'}$), in which the flow-splitting effect (dead flux effect) is discounted (Svarovsky, 1984).

In order to allow estimation of the reduced cut size, many authors suggested additional factors for Eq.(1) to account for the underflow-to-throughput ratio effect. Massarani (1997), for instance, put forth the following correlation for the prediction of reduced cut size:

$$\frac{d_{50}^{'}}{D_C} = K\left[\frac{\mu D_C}{Q(\rho_s - \rho)}\right]^{0.5} F(R_L)G(C_V) \tag{2}$$

where

$$F(R_L) = \frac{1}{1 + 1.73R_L} \tag{3}$$

$$G(C_V) = e^{(4.5C_V)} \tag{4}$$

R_L is the underflow-to-throughput ratio and C_V is the volumetric feed concentration. It should be noted that the effect of the underflow-to-throughput ratio and the influence of the solids concentration on cut size are both considered.

Massarani (1997) proposed Eq.(5) for prediction of the underflow-to-throughput ratio:

$$R_L = B\left(\frac{D_U}{D_C}\right)^C \tag{5}$$

where D_U is the underflow diameter and B and C are constants for a given cyclone design.

For Bradley's and Rietema's optimum designs, which are of interest in the present work, Massarani (1997) obtained the parameters shown in Table 1.

**Table 1: K, B and C parameters and Euler number for Bradley's
and Rietema's conventional designs.**

Design	K	B	C	Eu
Bradley	0.016	54.6	2.61	7000
Rietema	0.039	145	4.75	1200

For a specific hydrocyclone design, this author considers that the relationship between static pressure drop through the cyclone ($-\Delta P$) and dynamic pressure, calculated from the characteristic velocity u_c ($\rho u_c^2 / 2$), i.e., the Euler number, is constant, in according to Eq. (6):

$$Eu = \frac{-\Delta P}{\dfrac{\rho u_c^2}{2}} \qquad (6)$$

We emphasize that the aforementioned equations and parameters apply only to the conventional hydrocyclone, i.e., a nonfiltering device. Correlations like these have been estimated in this work, while considering the characteristics of the filtering medium.

Conical Filtration

As the conical sections of filtering hydrocyclones are permeable, a conical filtration occurs through them as the suspension circulates through the device. By applying the motion equation in cylindrical coordinates and Darcy's law to the conical wall, a simplified mathematical model for this filtration is deduced as shown below.

For an incompressible radial flow obeying Darcy's law across the filtering cone in steady state, as shown in Figure 2, the motion equation in cylindrical coordinates yields

$$-\frac{dP}{dr} = \frac{\mu}{K_m} \frac{Q_F}{A_L} \qquad (7)$$

where dP/dr is the pressure gradient through the porous wall, Q_F is the filtrate flowrate, K_m is the medium permeability, ε is the medium thickness and A_L is the lateral area of the cone surface. Alternatively, K_m and A_L might be expressed as follows:

$$R_m = \frac{\varepsilon}{K_m} \qquad (8)$$

where R_m is the filtering medium resistance and A_L is the lateral area of the cone surface, which might be expressed as a function of the lowest radius.

$$A_L = 2\pi r (L - L_1) + \frac{\pi}{2}(L - L_1)(D_c - D_{inf}) \qquad (9)$$

where L is the hydrocyclone length, L_1 is the length of the cylindrical section and D_{inf} is the lowest internal diameter of the cone.

Substituting Eq. (8) and Eq. (9) into Eq. (7):

$$-dP = \frac{\mu R_m}{\varepsilon} Q_F \frac{dr}{2\pi r (L - L_1) + \frac{\pi}{2}(L - L_1)(D_c - D_{inf})} \qquad (10)$$

For a uniform pore distribution (i.e., R_m does not depend on the position inside the cone) and an isothermal system (μ and ρ are constant), Eq. (10) can be integrated from ($D_{inf}/2$) to ($D_{inf}/2 + \varepsilon$). Doing this and isolating the filtrate flowrate (Q_F) we obtain Eq. (11):

$$Q_F = \frac{2\pi\varepsilon (L - L_1) \Delta P_m}{\mu R_m \ln\left(1 + \dfrac{4\varepsilon}{D_{inf} + D_c}\right)} \qquad (11)$$

Eq. (11) represents the volumetric filtrate flowrate obtained in a conical filtration as a function of the difference between the pressure directly applied to the filtering wall and the atmospheric pressure (ΔP_m) and the dimensions of the cone. It can be rearranged in order to allow estimation of the resistance of the filtering medium.

$$R_m = \frac{2\pi\varepsilon (L - L_1) \Delta P_m}{\mu Q_F \ln\left(1 + \dfrac{4\varepsilon}{D_{inf} + D_c}\right)} \qquad (12)$$

Thus, the relationship between the filtrate flowrates (Q_F) and pressure drops through the filtering cone ($-\Delta P_m$) is linear. The value of R_m may be estimated through linear regression of a data set. It might be argued that filter cake resistivity should be included in the formulation, analogous to flat filtration. Nevertheless, during the experiments it was verified that no cake is formed, owing to the high tangential velocity of the slurry within the hydrocyclones (Souza, 2000).
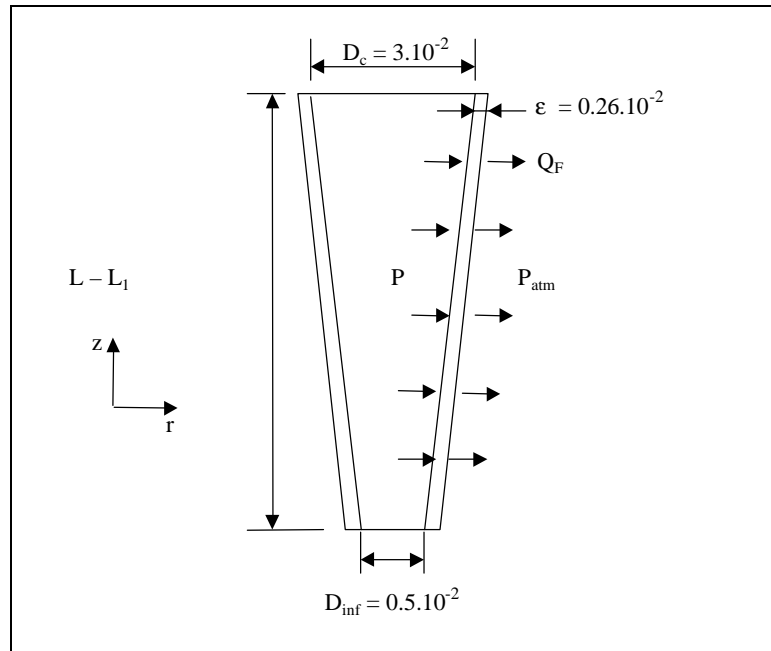
Figure 2: Filtrate radial flow across the filtering cone (dimensions in meters - not drawn to scale)

EXPERIMENTAL

Material

The particulate material used was pyrochlore (65% Nb_2O_5), which has a suitable density ($\rho_s = 4030$ kg.m^{-3}). The particle size distribution of the samples was determined by the gamma-ray attenuation unit. Am^{241} was the radioactive source utilized. The relationship between the beams counted by the equipment and the volumetric solids concentration (C_V) in a given suspension may be derived from Lambert's equation. Eq. (13), for example, was obtained for pyrochlore aqueous suspensions:

$$C_v = (42.74 \pm 0.55) \ln\left(\frac{I_o}{I}\right) \tag{13}$$

where I is number of the gamma-ray beams counted for a uniform suspension and I_o is the number of gamma-ray beams counted for pure water.

With the aid of an axial stirrer, the slurry was made uniform and its concentration calculated according to Eq. (13). The particles were allowed to settle further this time gravitationally, and the Stokes diameters and the cumulative mass fractions could be obtained by means of Eqs. (14) and (15), respectively. This procedure usually required approximately 25 minutes.

$$d_{Stk} = \sqrt{\frac{18\mu H}{(\rho_s - \rho_l)gt}} \tag{14}$$

$$X = \ln\left(\frac{I_o}{I_t}\right) \bigg/ \ln\left(\frac{I_o}{I}\right) \tag{15}$$

where d_{Stk} is the Stokes diameter, μ is the liquid viscosity, H is the position of measurement, t is the time of measurement, ρ is the liquid density, ρ_s is the solid density and I_t is the number of gamma-ray beams counted for a suspension at time t elapsed from the beginning of the settling.

In Figure 3 the fitting of the pyrochlore to the Rosin-Rammler-Bennet size distribution model is shown (Allen, 1997).

Hydrocyclones

Table 2 shows the dimensions of the hydrocyclones studied in this work (Bradley's and Rietema's designs).

The filtering hydrocyclones had cylindrical section diameter (D_C) of 3.10^{-2} m and underflow diameters (D_U) of 3.10^{-3}, 4.10^{-3} and 5.10^{-3} m. Three filtering cones R1, R2, R3, were made of sinter bronze for the hydrocyclone of Rietema's design. Besides, two cones of sinter bronze and one of polypropylene referred to as B1, B2 and P, respectively, were made in accordance with Bradley's design.
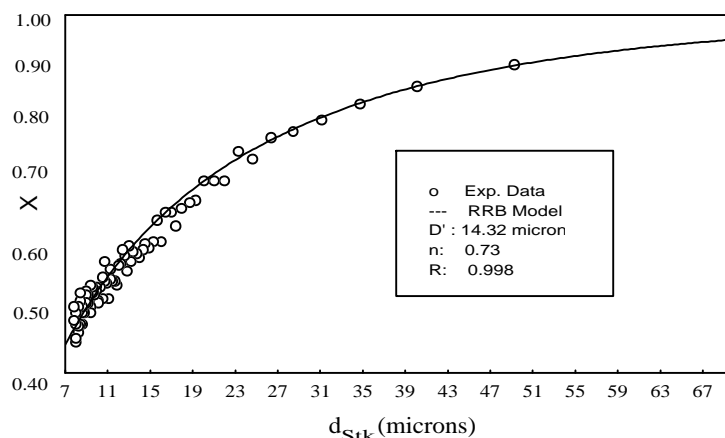
Figure 3: Size distribution of the pyrochlore particles.

Table 2: Dimensions of Rietema's and Bradley's hydrocyclones

	D_i/D_C	D_o/D_C	L/D_C	Angle
Rietema	0.28	0.34	5.00	20^0
Bradley	1/7	1/5	6.8	9^0

Experimental Apparatus and Procedure

Figure 4 illustrates the unit where the experiments were carried out. It basically comprises a well-stirred tank, whose volume was approximately 0.25 m^3, a 5 HP centrifugal pump, valves, a pressure gauge and the filtering hydrocyclone itself. The system was operated as follows: after filling the tank with the slurry, the stirrer was switched on in order to achieve efficient mixing. Then the pump was turned on and the pressure

drop was set to the desired value by either opening or closing the valves. The system was allowed to stabilize, a process which normally took about five minutes. Samples of all the streams, feed, overflow, underflow and filtrate, were then collected for further evaluation of mass flowrates, concentrations and particle size distributions. Gravimetric techniques were used to determine the mass flowrates. The properties of the fluid (μ and ρ) were estimated by measuring of the temperature of the suspension.
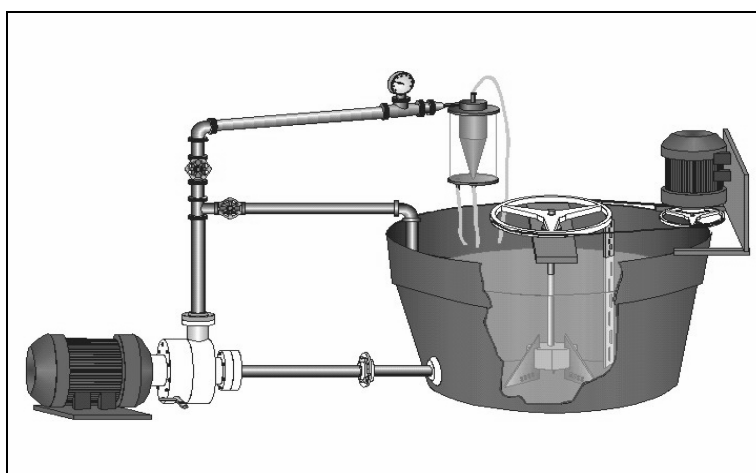

Figure 4: Experimental apparatus

Characterization of the Filtering Media

To apply Eq. (11) in determining of the filtering medium resistances (R_m), the filtering cones were fed with pure water at low flowrates at 25.5 ^{o}C. This was done to avoid the formation of vortices and to guarantee exertion of constant pressure on the wall. The experiments were carried out in a simple unit, similar to the one shown in Figure 4, but consisting of a peristaltic pump and a U-tube manometer. The underflow orifice and overflow tube were closed and the respective filtrate flowrates (Q_F) and pressure drops (ΔP_m) were varied and measured for each cone.

RESULTS AND DISCUSSION

In Table 3 the values of filtering medium resistance (R_m), obtained for the fitting of the experimental data to Eq. (11), are displayed the conventional hydrocyclones (without a filtering cone) were referred to as BC and RC for Bradley's and Rietema's designs, respectively.

The Table 3 demonstrates that similar ranges of the filtering medium resistances were used to Bradley and Rietema hydrocyclones. In the studied operational conditions, the P filtering hydrocyclone was the most permeable device while the B1 filtering hydrocyclone presented the smallest permeability.

Table 3: Filtering medium resistances (R_m) for the hydrocyclones

	Cone of Bradley's hydrocyclone				Cone of Rietema's hydrocyclone			
	B1	B2	P	BC	R1	R2	R3	RC
R_m (m^{-1})	$10.63.10^{11}$	$6.5.10^{11}$	$0.579.10^{11}$	∞	$6.37.10^{11}$	$4.95.10^{11}$	$4.54.10^{11}$	∞
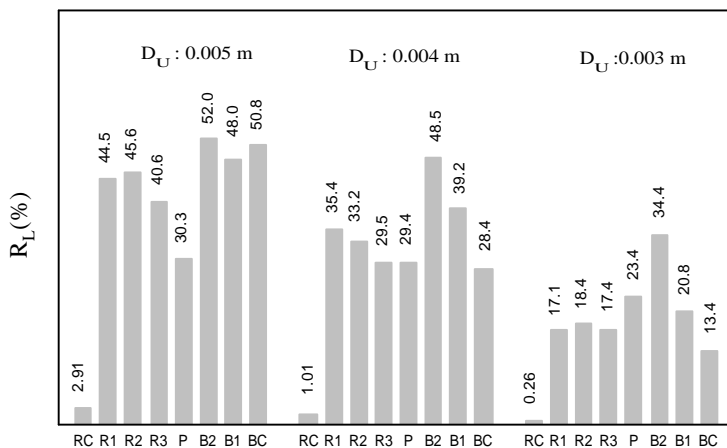
where

D_U	Diameter of the underflow
R_L	Underflow-to-throughput ratio
R1,R2,R3	Rietema's filtering hydrocyclones
RC	Rietema's conventional hydrocyclone
B1, B2, P	Bradley's filtering hydrocyclones
BC	Bradley's conventional hydrocyclone

Figure 5: Medium underflow-to-throughput ratio for all the hydrocyclones

The Underflow-to-Throughput Ratio

The underflow-to-throughput ratio in both designs was changed significantly by the filtering medium, as shown in Figure 5. By analyzing this figure, it is possible to conclude that the underflow-to-throughput ratios of both designs changed due to filtration. The more pronounced changes were seen

for which hydrocyclones Rietemas's design, which supplied more diluted underflow streams.

Through nonlinear regression, the experimental underflow-to-throughput ratios for both designs were correlated as a function of the underflow holes and filtering medium resistances. The correlations for Bradley's and Rietema's filtering hydrocyclones are represented by Eq. (16) and Eq. (17), respectively.

$$R_L = \frac{1}{1.69 - 8.66.10^{-6}(R_m D_C)^{0.5}} \left(\frac{D_U}{D_C}\right)^{\exp\left[-0.69 + 1.06.10^{-21}(R_m D_C)^2\right]} \quad (16)$$

where

$$0.1 \leq \left(\frac{D_U}{D_C} \right) \leq 0.167$$

$$0.174.10^9 \leq R_m D_C \leq 5.315.10^9$$

$$R_L = \left(\frac{D_U}{D_C} \right)^{1.66} \left(R_m D_C \right)^{0.092} \qquad (17)$$

where

$$0.1 \leq \left(\frac{D_U}{D_C} \right) \leq 0.167$$

$$1.362.10^9 \leq R_m D_C \leq 3.185.10^9$$

Feed Flowrate and Euler Number

Depending on the design, the filtering hydrocyclones behaved differently respective conventional devices. Figure 6 shows that while the volumetric feed flowrates decreased for Rietema's filtering hydrocyclones, there was an increase in this same variable for Bradley's filtering hydrocyclones, when compared with the conventional hydrocyclone.

As well as the changes in the volumetric feed flowrates, the filtering hydrocyclones had new values for the Euler numbers, as can be seen in Figure 7. Within the limits of the experimental region studied in this work, Rietema's filtering hydrocyclones had higher Euler numbers than the conventional device, while the Bradley's filtering hydrocyclones reductions in this same variable.

In accordance with experimental data, the Euler numbers for the Bradley's filtering hydrocyclones were mainly influenced by the resistance of the filtering medium and the underflow-to-throughput (Eq. (18)), while this same variable for Rietema's filtering hydrocyclones was only dependent on the Reynolds number and the underflow dimension (Eq. (19)).
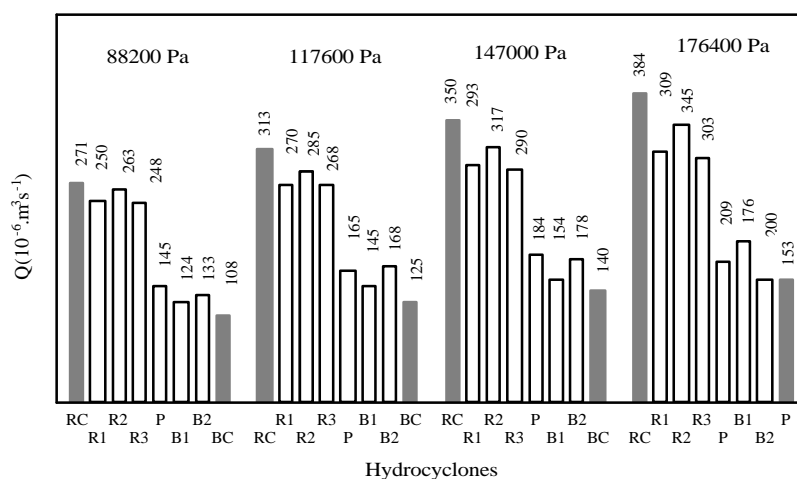

Figure 6: Volumetric feed flowrates at different pressure drops (D_U: 0.005 m)
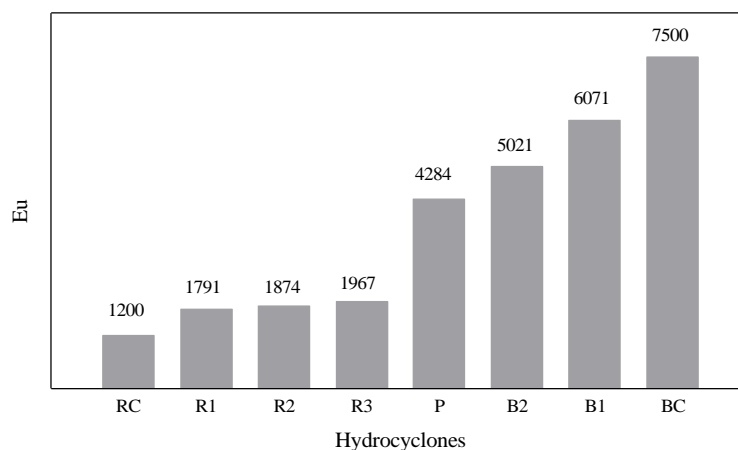

Figure 7: Euler numbers for the hydrocyclones

$$Eu = \frac{1}{\left[0.0119 + 0.0296R_L \sqrt{\dfrac{16\rho\varepsilon(L-L_1)}{\pi\mu D_C R_m \ln\left(1+\dfrac{4\varepsilon}{D_C+D_{inf}}\right)}} \right]^2} \qquad (18)$$

where

$$0.174.10^9 \le R_m D_C \le 5.315.10^9$$

$$Eu = Re^{(0.63)}\left(\frac{D_U}{D_C}\right)^{(-0.73)} \qquad (19)$$

where

$$10221 \le Re \le 16394$$

$$0.1 \le \left(\frac{D_U}{D_C}\right) \le 0.167$$

Overall Efficiency

Changes in the underflow-to-throughput ratios affected overall efficiency in both designs that were employed in this study, as shown in Figure 8.

The overall efficiency of Rietema's filtering hydrocyclones increased more than that of the conventional device. This characteristic behavior of overall efficiency occurred due to the increase in the values of the underflow-to-throughput ratio, which were responsible for the higher drag of solids by the underflow stream. For Bradley's filtering hydrocyclones the opposite occurred because the reduction in the underflow-to-throughput ratio caused lower overall efficiencies than that of the conventional hydrocyclone.
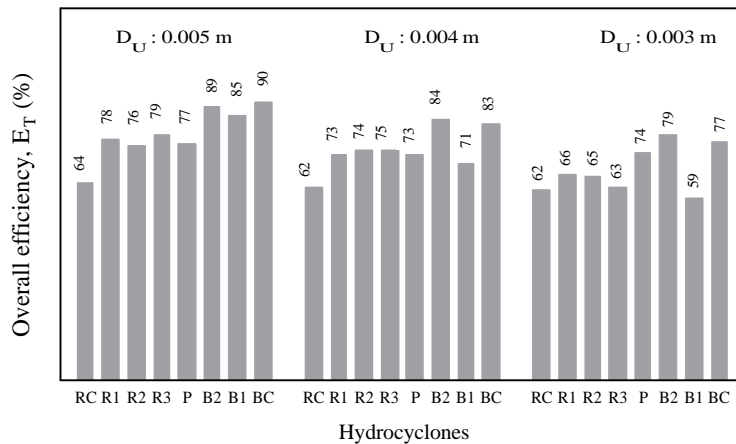

Figure 8: Overall efficiencies of the hydrocyclones

Based on the experimental data collected on the filtering hydrocyclones, Eq. (20) and Eq. (21) were proposed for Bradley's and Rietema's designs, respectively. These expressions elucidate how the well-defined of separation changes as a function of volumetric feed flowrate and underflow-to-throughput ratio.

$$\frac{d'_{50}}{D_C} = (0.064 \pm 0.004)\left[\frac{\mu D_C}{Q(\rho_s - \rho)}\right]^{0.5}$$
$$(1 - R_L)^2 \exp(4.5C_V) \qquad (20)$$

$$\frac{d'_{50}}{D_C} = (0.036 \pm 0.001)\left[\frac{\mu D_C}{Q(\rho_s - \rho)}\right]^{0.5}$$
$$\frac{1}{1 + (0.51 \pm 0.12)R_L}\exp(4.5C_V) \qquad (21)$$

In this context, it could be verified that the main modifications in reduced cut sizes occurred due to the new values of underflow-to-throughput ratio. In both filtering hydrocyclones, this variable reflects all the influences of the filtration process, as observed in function $F(R_L)$.

CONCLUSIONS

The experimental results obtained with the filtering hydrocyclones under the same operational conditions as those for the corresponding conventional devices, allow the following conclusions to be drawn.

The performance of the hydrocyclones of Bradley's and Rietema's designs is significantly influenced by the filtering medium. The underflow-to-throughput ratios of both filtering devices underwent changes in relation to the corresponding conventional devices increasing for Rietema's filtering hydrocyclone and decreasing for Bradley's filtering hydrocyclone. While Rietema's filtering hydrocyclones had a lower volumetric feed flowrate than the conventional device, Bradley's filtering hydrocyclones showed increases in this same variable. While the Euler numbers for Rietema's filtering hydrocyclones increased move under the same operational conditions, than that of the conventional device, for the Bradley's filtering hydrocyclones they decreased. In both designs, overall efficiency was influenced by the underflow-to-throughput ratio. For Rietemas's filtering hydrocyclones the underflow-to-throughput ratio contributed to the increase overall efficiency. The overall efficiency of the Bradley's filtering hydrocyclones decreased compared to the conventional device, due to the reduction in solids in the underflow stream. Filtration and design were equally important at the same degree for understanding the separation process in the filtering hydrocyclone.

NOMENCLATURE

A_L	lateral area of the cone surface	(m^2)
B and C	parameters in Eq. (5)	(-)
C_V	volumetric solid concentration	$(m^3_{solid}/ m^3_{suspension})$
D_C	diameter of the cylindrical section of the hydrocyclone	(m)
D_i	inlet diameter of the hydrocyclone	(m)
D_{inf}	lowest internal diameter of the filtering cone	(m)
D_O	overflow tube diameter	(m)
D_U	underflow orifice diameter	(m)

d_{Stk}	Stokes diameter	(m)
d_{50}	cut size	(m)
d_{50}'	reduced cut size	(m)
Eu	Euler number	(-)
g	gravity	(-)
H	position of gamma-ray measurement	(m)
I	gamma-ray beams counted for suspension	(-)
I_o	gamma-ray beams counted for pure water	(-)
I_t	gamma-ray beams counted for suspension as a function of time	(-)
K	parameter in Eq.(1) and Eq.(2)	(-)
K_m	filtering medium permeability	(m^2)
l	vortex finder length	(m)
L	hydrocyclone length	(m)
L_1	length of the cylindrical section of the hydrocyclone	(m)
P	pressure of gas inside the filtering cone	$(kg\ m^{-1}s^{-2})$
P_{atm}	atmospherie pressure	$(kg\ m^{-1}s^{-2})$
Q	volumetric feed flowrate	$(m^3\ s^{-1})$
Q_F	volumetric filtrate flowrate	$(m^3\ s^{-1})$
Re	Reynolds number	(-)
R_L	underflow-to-throughput ratio	(-)
R_m	filtering medium resistance	(m^{-1})
t	time	(s)
u_c	speed of the suspension in the cylindrical area	$(m\ s^{-1})$
X	cumulative mass fraction	(-)

Greek Letters

ε	filtering medium thickness	(m)
ΔP	pressure drop between the feed volumetric and overflow streams	$(kg\ m^{-1}s^{-2})$
μ	liquid viscosity	$(kg\ m^{-1}s^{-1})$
θ	included angle of the cone	(-)
ρ, ρ_s	liquid and solid density, respectively	$(kg\ m^{-3})$

ACKNOWLEDGMENTS

REFERENCES

Allen, T., Particle Size Measurement, 5th ed., London: Chapman and Hall, 524p. (1997).

Barrozo, M.A.S., Damasceno, J.J.R. and Lanna, A.E., Estudo do Desempenho de um Hidrociclone Filtrante, Revista Ciência & Engenharia, 1, pp. 175-186 (1992).

Massarani, G., Fluidodinâmica em Sistemas Particulados, Rio de Janeiro: Editora UFRJ, (1997).

Rietema, K., Performance and Design of Hydrocyclone. Chemical Engineering Science, 15, pp. 298-325 (1961).

Souza, F.J., Vieira, L.G.M., Damasceno, J.J.R. and Barrozo, M.A.S., Analysis of the Influence of the Filtering Medium on the Behaviour of the Filtering Hydrocyclone, Powder Technology, vol. 107, pp. 259-267 (2000).

Svarovsky, L., Solid-liquid Separation, London-UK: Butterworths, (1981).

Svarovsky, L., Hydrocyclones, New York: Holt, Rinehart and Winston (1984).